The Amazonian Boundary Layer and Mesoscale Circulations

A. K. Betts,[1] G. Fisch,[2] C. von Randow,[3] M. A. F. Silva Dias,[4] J. C. P. Cohen,[5] R. da Silva,[6] and D. R. Fitzjarrald[7]

The interactions between the Amazonian boundary layer, the surface, atmospheric convection, aerosols, and larger-scale circulations are complex. The field experiments in Amazonia have provided rich insights into the daytime and nighttime boundary layer in different regions and seasons over both forest and pasture and into the coupling between the surface fluxes, the boundary layer, precipitation, and cloud radiative forcing. We discuss the typical diurnal cycle of Amazonian convection, the self-organization into mesoscale systems in different synoptic regimes, and the role of forest and river breeze circulations. We review the coupling between aerosols, smoke, and convection in the dry season; ozone transports by deep convection; and microphysical and electrical impacts on convection.

1. INTRODUCTION

Understanding the complex interaction of clouds, rain, and the biosphere in the Amazon was the reason for the Large-Scale Atmosphere-Biosphere Experiment in Amazonia (LBA) experiment [*Silva Dias et al.*, 2002a]. The focus of this chapter is the Amazonian boundary layer (BL) and its coupling with the surface, atmospheric convection, and larger-scale circulations. An early BL study using radiosoundings and tethered balloons was made during the Global Tropospheric Experiment Amazon Boundary Layer Experiment (ABLE 2B) [*Martin et al.*, 1988] at a tropical forest site near Manaus, followed by a longer study at contrasting forest and pasture sites during the Rondônia Boundary Layer Experiment (RBLE) [*Nobre et al.*, 1996]. During the LBA experiment, two main field campaigns took place to characterize the structure and evolution of the BL [*Fisch et al.*, 2004]. The first was during the wet season in early 1999: the Wet-Season Atmospheric Mesoscale Campaign (WETAMC) and the coincident Tropical Rainfall Measuring Mission (TRMM). The second field program was during the dry-to-wet transition season, September to November 2002; it also had two components, the study of Radiation, Cloud, and Climate Interactions (LBA-RACCI) and the study of the interaction of Smoke Aerosols, Clouds, Rainfall and Climate (LBA-SMOCC).

The surface energy partition is controlled by the availability of water for evaporation, which depends on precipitation, soil moisture storage, and the vegetation cover [*da Rocha et al.*, this volume]. Over the Amazon Basin, precipitation comes mostly from deep convection, which is coupled not only to the surface BL, surface topography, and heterogeneities (section 3.7) but also to circulations on continental and global scales [*Nobre et al.*, this volume]. Deep convection is also self-organizing on the mesoscale along cold pool outflow boundaries (section 3). *Horel et al.* [1989] described, using reanalysis data and outgoing long-wave radiation

[1]Atmospheric Research, Pittsford, Vermont, USA.
[2]Instituto de Aeronáutica e Espaço, São José dos Campos, Brazil.
[3]Instituto Nacional de Pesquisas Espaciais, São José dos Campos, Brazil.
[4]Department of Atmospheric Sciences, University of São Paulo, São Paulo, Brazil.
[5]Departamento de Meteorologia, Universidade Federal do Pará, Belém, Brazil.
[6]UFPA-LBA Santarem, Alter do Chão, Brazil.
[7]Atmospheric Sciences Research Center, University at Albany, State University of New York, Albany, New York, USA.

Amazonia and Global Change
Geophysical Monograph Series 186

10.1029/2008GM000725

from satellites, the movement of deep convection over South America, which impacts the rainfall distribution over the tropical Americas. *Machado et al.* [2004] showed the climatological aspects of the seasonal and diurnal variability of convection over Amazonia and its links to different vegetation types and large-scale forcing, using long-time series of radiosonde and satellite data for cloud cover (from the International Satellite Cloud Climatology Project (ISCCP)) and the normalized difference vegetation index. Figure 1 shows that July is the driest month for the majority of Brazil (Figure 1a). The dry season duration in Figure 1b shows two minima, one over west Amazonia, associated with the monsoon circulation and persistent convection, and another in the south of Brazil, associated with the penetration of cold fronts. We shall give considerable emphasis to studies in SW Amazonia (specifically Rondônia and the Rio Madeira Basin) in section 2 because of the large seasonal cycle.

Prior to LBA, the Rondônia Boundary Layer Experiment (RBLE 3) collected data from representative regions of forest and deforested pasture in the Ji-Paraná region of Rondônia during the 1993 dry season [*Nobre et al.*, 1996]. Nobre et al. noted the much deeper daytime BL over the pasture site, where the surface sensible heat flux is roughly double that over the forest in the dry season. In contrast, the nighttime BL is deeper over the aerodynamically rougher forest. However, simple one-dimensional mixed layer models failed to capture the diurnal cycle of the growth of the daytime unstable BL and underestimated the large differences in the afternoon BL depth between forest and pasture [*Fisch et al.*, 1996]. Fisch et al. suggested that the horizontal heterogeneity and mesoscale circulations must be important, both within the deforested area, where strips of forest remain (spacing of the order of 5 km), as well as between the forest and pasture regions, a distance of 90 km.

2. WHAT IS DISTINCTIVE ABOUT THE AMAZONIAN BOUNDARY LAYER?

Over land, the boundary layer goes through a strong diurnal cycle [e.g., *Betts*, 2003] as it links the heated surface to the atmosphere during the day and uncouples from the atmosphere at night. Since the BL couples the atmosphere to the surface on the daily timescale, its structure depends both on differences in the surface, the roughness and the availability of water for evaporation, and differences in the overlying atmosphere. Over the moist forested Amazon Basin, the surface water storage is large (available soil water storage may approach 800 mm, see *Hodnett et al.* [1996] and Figure 4), and the surface vegetative conductance is correspondingly large (typical values are around 30 mm s^{-1} [*Wright et al.*, 1996]). Consequently, the drop in relative humidity across the leaf at the surface (which is related to the height of the lifting condensation level) is small, and so daytime cloud base heights are also small, typically reaching only 1000 m [*Betts et al.*, 2002a], somewhat more in the dry season [*Nobre et al.*, 1996]. In addition, the cooled nighttime stable BL generally saturates and is about 300 m deep over the aerodynamically rough forest [*Nobre et al.*, 1996]. In southern Amazonian regions, where there is a strong annual cycle of precipitation, there is sufficient available storage of water in

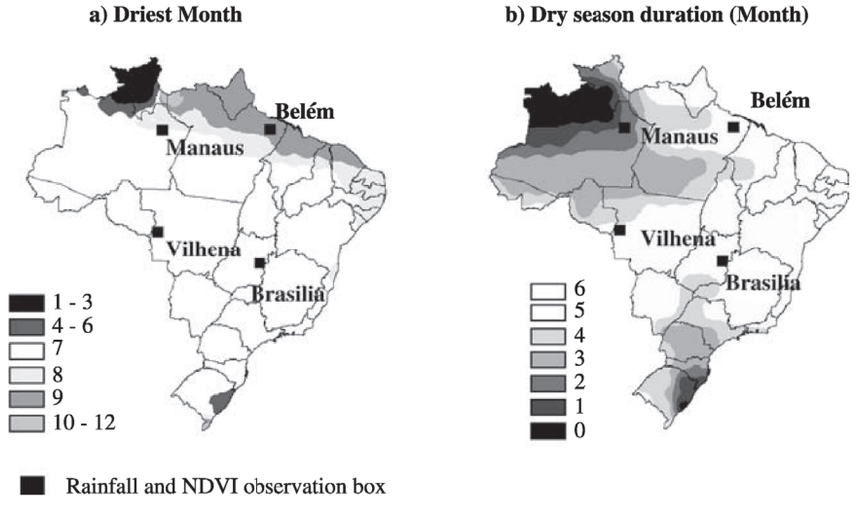

Figure 1. (a) Driest month (month of minimum high cloud cover). (b) Dry season duration defined using high cloud cover. Adapted from *Machado et al*. [2004], reprinted with permission of Springer-Verlag.

the soil in forested areas that the drop in evaporation in the dry season and corresponding deepening of the dry adiabatic subcloud layer is small (less than 20–30% [*da Rocha et al.*, this volume]). In contrast, in deforested regions in Rondônia, where available soil moisture is much reduced, the evaporation falls sharply in the dry season, and the subcloud layer depth may reach nearly 2000 m in the afternoon.

Over most of the Amazon Basin, the overlying tropical atmosphere is convectively coupled. In the rainy season, the entire troposphere is linked to a single moist adiabat, near-neutral stability for deep convection, with a minimum saturation equivalent potential temperature close to the freezing level in the middle troposphere. In the dry season in the southern Amazon, when there is subsidence aloft, a weak inversion caps a layer of shallow cumulus, and only the lower troposphere is convectively coupled on many days. However, in all seasons, a partly cloudy convective boundary layer, which is coupled to the surface, controls the surface radiative energy budget. We first look at atmospheric differences between seasons and then at the seasonal differences in the surface processes between forest and pasture in Rondônia.

2.1. Monthly Mean Atmospheric Differences Between Wet and Dry Seasons

The seasonal cycle over SW Amazonia is driven by the large-scale circulation [see *Nobre et al.*, this volume]. Figure 2a shows the monthly mean vertical omega field (vertical velocity in pressure units) over the Rio Madeira Basin, derived from hourly model data from the European Centre for Medium-Range Weather Forecasts (ECMWF) 40 Year Reanalysis (ERA-40) [*Betts and Viterbo*, 2005]. Both months show convergence and ascent near the surface, but in the rainy season, mean ascent is positive throughout the troposphere, peaking around 300 hPa. This destabilization is, of course, balanced by heavy convective precipitation. During the dry season, subsidence dominates, peaking at around 700 hPa, and this suppresses deep convection. The result is the dramatic difference in the mean relative humidity (RH) of the troposphere, shown in Figure 2b (as well as in precipitation and cloud cover, not shown). In February in the rainy season, RH is above 70% in the lower troposphere, while in August, mean RH falls steeply above 700 hPa to about 20% in the middle troposphere.

As a result of this different tropospheric forcing, the stability of the atmosphere with regard to moist convection is very different in the two seasons, as shown in Figure 3, which shows the mean vertical profiles of equivalent potential temperature, θ_E, and θ_{ES} its saturation value, which represents temperature in this moist adiabatic reference system. The

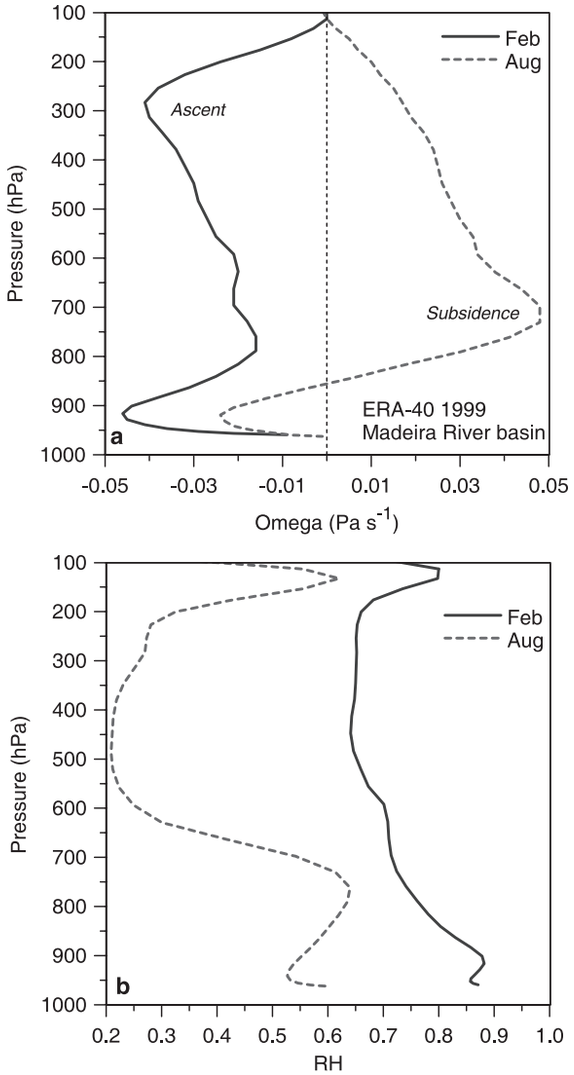

Figure 2. (a) Vertical profiles of monthly mean vertical velocity field for February and August 1999 for Rio Madeira Basin from ERA-40. (b) Same as Figure 2a but for RH profiles.

dotted lines represent moist adiabatic parcel ascent from the 30-hPa layer near the surface. In February, this lifted parcel is buoyant through much of the troposphere. In contrast, in August, the daily mean parcel is never buoyant if lifted. Indeed, in the dry season, the shallow cumulus convection occurs only in the daytime, when the surface heating is strong, and it is generally trapped below the temperature inversion from 700 to 600 hPa, which, in turn, is maintained by the subsidence shown in Figure 2a. Rain events in the dry season typically occur with the intrusion of cold fronts from the extratropics [*Fisch et al.*, 2004]. Note that the subsidence in Figure 2a peaks at the base of the inversion, where

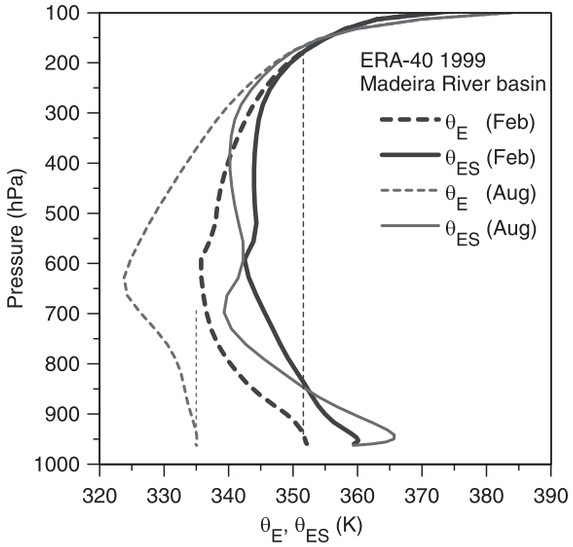

Figure 3. Monthly mean vertical profiles of θ_E and θ_{ES} for February and August 1999 for Rio Madeira Basin from ERA-40 reanalysis.

the shallow cumulus detrain their liquid water and cool the atmosphere.

2.2. Surface Seasonal Differences Between Forest and Pasture

Forest and pasture respond differently to similar atmospheric forcing [*Culf et al.*, 1996]. *von Randow et al.* [2004] show seasonal comparisons between pasture (Fazenda Nossa Senhora) and forest (Rebio Jaru) sites in Rondônia. Monthly averages of air temperature and specific humidity and monthly totals of rainfall measured over the pasture and forest sites during the period February 1999 to September 2002 are shown in Figure 4a. The range in monthly mean air temperature is small, and it is not easy to identify a clear seasonal pattern. Strong precipitation events in January–February and penetrating cold fronts in June–July influence the averages in some years. On the other hand, a clear drop in specific humidity and a drastic reduction in rainfall during the dry seasons are observed at both sites. Rainfall amounts were higher at the forest site (2000–2400 mm a^{-1}) than at the pasture site (1400–2000 mm a^{-1}), but it is unclear whether these differences are truly representative of larger areas [*von Randow et al.*, 2004]. However, *Ferreira da Costa et al.* [1998] compared rainfall from contrasting sites (forest and pasture) at Rondônia during four rainy seasons (December–February) from 1992 to 1995 and also found 28% greater rainfall over forest than over pasture. *Fisch et al.* [2007] analyzed the spatial variation of the convective rainfall in this region, using the TRMM rain gauge network. They used a statistical model of a rainfall event and concluded that at a distance greater than 5 km, the measured rainfall from typical convective cells had a poor correlation (0.2 ~ 0.4). The specific humidity is also always higher in the forest area, with average values ranging from 15.8 g kg^{-1} in the dry seasons to 17.5 g kg^{-1} in the wet seasons, while at the pasture, the average values are 13.4 and 16.0 g kg^{-1} in the dry and wet seasons, respectively.

Figures 4b and 4c show the storage of water for the layers from 0 to 2 m and 2 to 3.4 m, respectively, in the soil profile. Both forest and pasture show a very pronounced seasonal cycle, with much larger dry season decreases in the forest than the pasture, especially in the lower layer, where the deep root extraction is much greater in the forest [*von Randow et al.*, 2004; *Negrón Juárez et al.*, 2007]. Consequently, over the forest, the surface Bowen ratio, given by ratio BR = $H/\lambda E$ (where H and λE are the surface sensible and latent heat fluxes respectively) varies little, increasing slightly in the range 0.3–0.4 from wet to dry seasons. However, over the pasture, where there is little deep root extraction, BR increases from about 0.4 in the rainy season [*Betts et al.*, 2002a] to 0.65 in August [*von Randow et al.*, 2004]. *Galvão and Fisch* [2000] reported BR increases from 0.21 to 0.3 over the forest and from 0.32 to 0.76 over the pasture between the wet and dry seasons. There remains considerable uncertainty in these surface flux estimates because of the lack of energy balance closure using eddy correlation methods [*von Randow et al.*, 2004]. In a later study combining eddy correlation and scintillometry measurements, *von Randow et al.* [2008] show that the eddy fluxes do not fully capture the spatial variability of turbulence, especially at low frequencies. As this affects both H and λE, it is likely that the percent uncertainty in the Bowen ratio is smaller than in the individual fluxes.

Over forest sites, where deep soil water is available even through a dry season, evapotranspiration depends largely on the surface net radiation [*Negrón Juárez et al.*, 2007; *Hasler and Avissar*, 2007]. The surface radiative budget is thus a critical component of the surface forcing of the BL. Figure 5 (top) [*von Randow et al.*, 2004] shows the mean annual cycle of surface albedo; Figure 5 (bottom) shows the net short-wave flux, S_n, net long-wave flux, L_n, and net all-wave radiation flux, R_n, over forest and pasture. The solar radiation reflected by the pasture is larger throughout the year and reaches a peak early in the dry season, much earlier than the lower forest peak in albedo.

Several factors contribute to the seasonal variation in incident solar radiation (not shown): solar zenith angle, cloud cover, which peaks in the rainy season, and smoke from burning during the dry season. However, the albedo differ-

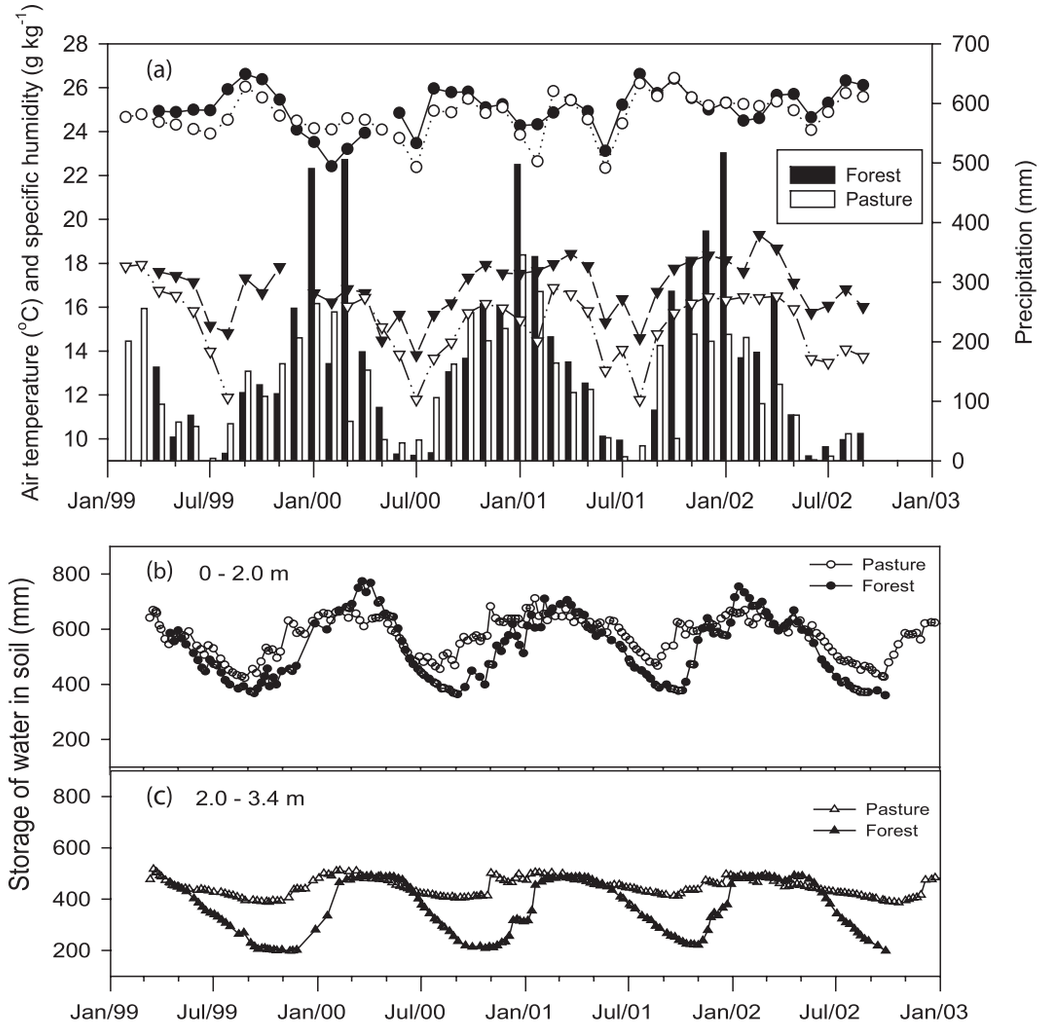

Figure 4. (a) Monthly averages of air temperature (circles), specific humidity (inverted triangles), and monthly totals of precipitation (columns) measured over the forest (represented by solid symbols) and pasture (represented by open symbols) from February 1999 until September 2002. Storage of water in the soil at forest and pasture sites for the layers from (b) 0–2 m and (c) 2–3.4 m deep. Adapted from *von Randow et al*. [2004], reprinted with permission of Springer-Verlag.

ence dominates the difference in S_n between forest and pasture. Outgoing L_n has a large seasonal variation, peaking in August when the atmosphere is dry (Figure 2b) and cloud cover is a minimum. Outgoing L_n is slightly larger over the pasture primarily because of warmer mean daytime temperatures. Throughout the year, R_n is greater over forest because of its lower albedo and slightly smaller outgoing long-wave flux. The mean annual reduction in R_n over the pasture is 13.3% [*von Randow et al.*, 2004], smaller than the 20.4% given for the boreal forest by *Betts et al.* [2007], where snow cover also reduces R_n over grass in late winter.

2.3. Diurnal Cycle of the Amazonian BL

The daytime convective BL over Amazonia is rarely cloud-free, so the depth of the mixed layer below cloud base, the lifting condensation level and the near-surface RH are all tightly coupled [see *Betts et al.*, 2006]. Near-surface RH is strongly influenced by the availability of water for evaporation, so forest sites where rooting is deep (Figure 4) and pasture sites show larger differences in the dry season than in the wet season. Afternoon mixed layer heights range from 700 to 1100 m in the rainy season over forest and pasture, when

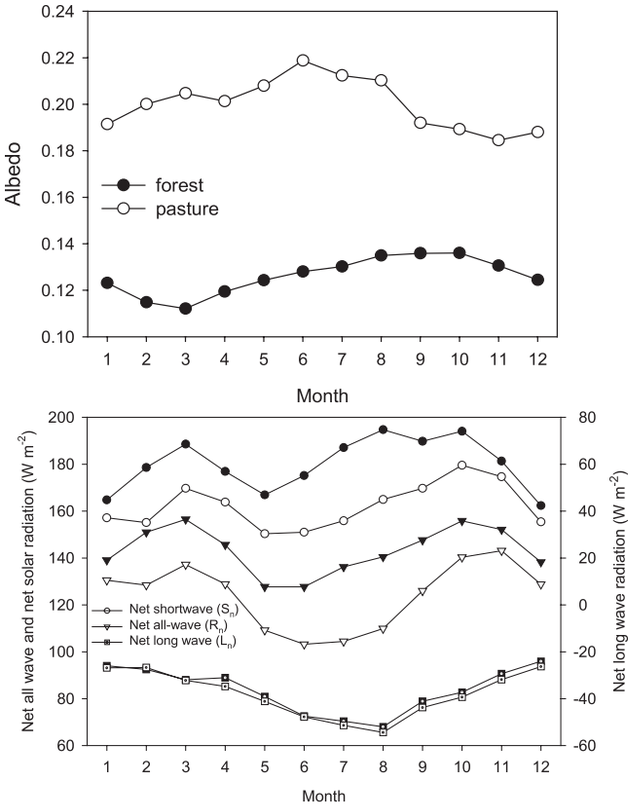

Figure 5. Monthly averages of (top) surface albedo and (bottom) net short-wave radiation (S_n, circles), net long-wave radiation (L_n, squares) and net all-wave radiation (R_n, inverted triangles) over forest (solid symbols) and pasture (open symbols) during 1999–2002. Adapted from *von Randow et al*. [2004], reprinted with permission of Springer-Verlag.

Bowen ratios are low and RH is high [*Fisch et al.*, 2004; *von Randow et al.*, 2004]. In the dry season, strong subsidence (Figure 2a) brings dry air into the BL, and evaporation is reduced over the pasture in Rondônia, so mixed layer depths are much larger and can reach 2000 m over the pasture. *Betts et al.* [2002a] and *Strong et al.* [2005] discuss the surface diurnal cycles of temperature, humidity, lifting condensation level, equivalent potential temperature, surface fluxes, and BL cloud for easterly and westerly regimes (see section 3.3) at the Rondônia pasture site in the 1999 rainy season. They show that the downward solar radiation and the fluxes of sensible and latent heat are lower for the westerly wind regime, which has more stratiform cloud but has a higher water vapor mixing ratio with a weaker diurnal cycle. The easterly wind regime shows an early morning maximum of mixing ratio, followed by a fall to a minimum in the afternoon, as the cumulus clouds mix water vapor up and out of the subcloud layer more rapidly than is provided by surface evaporation. As the rainy season progresses throughout January and February 1999, there is a steady transition toward cloudier conditions and lower surface fluxes. Daytime surface Bowen ratio for this pasture site is about 0.4 and falls slightly as the rainy season progresses. Typically, in the afternoon, evaporatively driven downdrafts from convective rainbands transform the boundary layer. The fall of equivalent potential temperature in the boundary layer is about 10K and is similar for both regimes, but the boundary layer cooling by individual convective events during the westerly regimes is reduced because the subcloud layer is shallower on average, as rain events are weaker but more frequent. This boundary layer modification by rainbands is rather similar to that seen in other moist convection regimes in the tropics (e.g., in Venezuela [*Betts*, 1976]).

Figure 6 compares the seasonal cycle of the diurnal cycle for the near-surface variables for the Rondônia pasture and forest sites during 2001, using data from *von Randow et al.* [2004]. Note that the temperature, T, and relative humidity data, RH, are from Vaisala HMP35A instruments, mounted at very different heights: 8.3 m over the pasture and 60 m over the forest floor, well above the mean canopy height of 35 m [*von Randow et al.*, 2004]. The "wet" season mean is January, February, and March; the "dry" season here is simply August, when mean subsidence is strongest over Rondônia; and the "dry-to-wet" transition is an average of September and October. Although the mean temperature in Figure 6a varies little over the year, the diurnal amplitude of temperature doubles between the wet and dry seasons, as the atmosphere gets drier and less cloudy, and the outgoing net long-wave radiation, which is a primary driver of the diurnal temperature range [*Betts*, 2006], doubles (see Figure 5). The forest data (at 60 m) are warmer than the pasture (at 8.3 m) in the rainy season, but the pasture becomes warmer in the daytime in the dry season with a greater increase in diurnal range.

The diurnal moisture structure in Figure 6b shows the seasonal fall of water vapor mixing ratio, Q, between wet and dry seasons and the rapid recovery by the transition season. The forest always has a greater mixing ratio than the pasture [*von Randow et al.*, 2004]. For Figure 6, a low bias of 4.3% near saturation at the pasture site was corrected, but it is possible that part of the humidity difference between sites is still instrumental, as these instruments are only calibrated to a few percent in RH. Indeed, absolute calibration of humidity instruments is difficult in these very moist tropical environments [*Betts et al.*, 2002c]. Away from the rainy season, mean mixing ratio rises steeply from a morning minimum at sunrise, when the atmosphere is saturated at the surface (Figure 6d), as evaporation is trapped in the stable nocturnal BL.

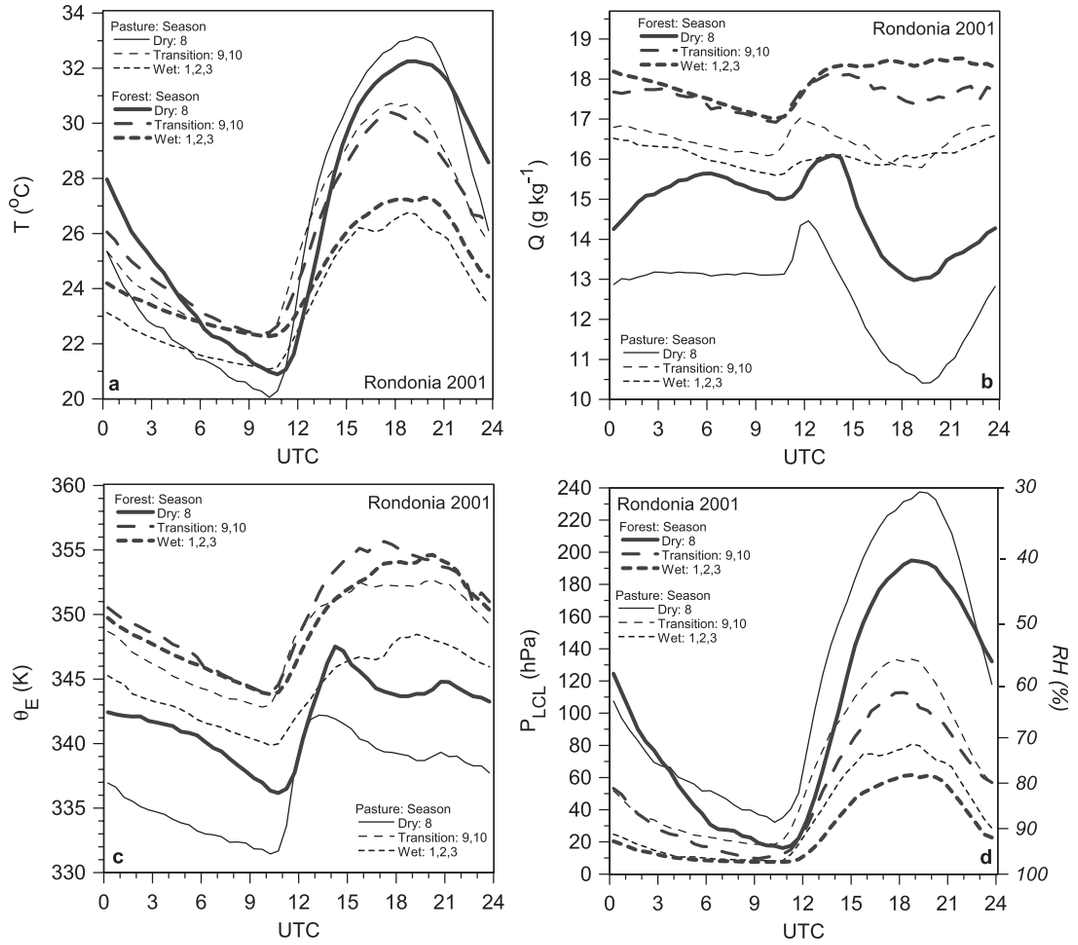

Figure 6. Diurnal cycle of (a) *T*, (b) *Q*, (c) θ_E, and (d) P_{LCL} for Rondônia forest and pasture sites in the wet and dry seasons and the transition from dry to wet in 1999.

Only a few hours after sunrise, the deepening mixed layer breaks through the nocturnal inversion and mixes with the residual layer above, and *Q* stops rising, as BL clouds transport water vapor out of the mixed layer. In the dry season, this coupling with the convective cloud layer above leads to a strong fall of *Q* following the morning peak and a weaker fall in equivalent potential temperature θ_E, shown in Figure 6c. Over the forest, θ_E is larger than over the pasture, as it depends mainly on *Q*. In the wet season, mean θ_E rises during the daytime, until the onset of deep convection brings lower θ_E air from higher levels into the subcloud layer in downdrafts [*Betts et al.*, 2002a]. Note that the mean θ_E over the forest reaches a slightly higher mean peak in 2001 in the transition season, when deep convection is strongest (see section 3.5).

Finally, Figure 6d shows the pressure height from the surface to the lifting condensation level (LCL), P_{LCL} (the different measurement heights above the surface have been added). As discussed at the beginning of this section, the LCL over Amazonia is a good estimate of daytime cloud base and the depth of the mixed layer. The corresponding near-surface RH is shown on the right-hand scale (with slight approximation). In August 2001, mean afternoon cloud base reaches nearly 240 hPa (2100 m) above the pasture; while in the wet season, afternoon cloud base height is only 60 hPa (545 m) over the forest. Such a low cloud base is more typical of the tropical oceans, so this has led to the description of the Amazon Basin as a "green ocean."

2.4. Nocturnal Boundary Layer

Nocturnal boundary layer (NBL) development is different between dry and wet seasons and between forest and pasture. The greater surface stress over the forest surface

generates a deeper NBL through enhanced turbulent mixing [*Nobre et al.*, 1996]. The long-wave radiative cooling of the surface is much larger in the dry season because of the lower humidity of the overlying atmosphere and reduced nocturnal cloud cover [*Betts*, 2004, 2006], and this leads to a more stable NBL [*R. M. N. dos Santos*, 2005]. In addition, the NBL develops from an afternoon BL, which typically has a deep "well-mixed" dry adiabatic structure in the dry season, but develops from a disturbed rain-cooled structure closer to a wet adiabatic temperature profile in the rainy season. Consequently, it is easier to define the depth of the NBL in the dry season, when the surface cooling is larger and the residual BL above is closer to a dry adiabat.

A comparison between the NBL over the forest (Rebio Jaru) and pasture (Fazenda Nossa Senhora) in Rondônia for the August 1994 RBLE 3 dry season was given by *R. M. N. dos Santos* [2005]. Using primarily tethered balloon data to define the height and temperature profile of the NBL, she showed that the difference, $\Delta\theta$, between the surface and NBL top (a measure of the strength of the NBL) reached about 11K at 0500 local solar time (LST) (before sunrise) over both forest and pasture. However, at 0500 LST the NBL depth was typically 30% greater over the rougher forest (420 ± 84 m) than over the pasture (320 ± 46 m). This difference is consistent with the theoretical analysis of NBL depth and strength, based on reanalysis model data by *Betts* [2006]. Another factor that may contribute to a deeper forest NBL is that the sensible heat flux reverses sign, and the NBL growth starts almost 1 hour earlier over the forest than over the pasture in Rondônia [*Oliveira and Fisch*, 2000]. *R. M. N. dos Santos* [2005] also analyzed three data sets collected during the TRMM-LBA rainy season in Rondônia at the same forest and pasture sites and a third transitional forest-pasture site at Rolim de Moura. In the rainy season, the NBL is similar at all three sites. Compared to the dry season, the NBL depth is shallower, typically about 240 m before sunrise, and much weaker in strength, with $\Delta\theta$ typically in the range of 3.5–4K [*R. M. N. dos Santos*, 2005], because the nighttime long-wave cooling is much less in the humid wet season. The near-surface layer usually saturates at night in the rainy season. The NBLs during the wet season were mostly weakly stable over forest and pasture. The most intermittent turbulence, associated with the greatest Monin-Obukhov (z/L) stability parameter, was seen at the transitional forest-pasture site [*R. M. N. dos Santos*, 2005].

Low-level nocturnal jets are commonly observed in Rondônia: in the RBLE 3 dry season on about 80% of the days and in the February 1999 wet season experiment on about 60% of the days [*R. M. N. dos Santos*, 2005]. Jet speeds are similar over forest and pasture and in both dry and wet seasons (mean 7.6 ± 1.9 m s^{-1}, sample size $N = 94$ soundings); but the height of the jet maximum was typically lower in the dry season (470 ± 165 m, $N = 29$) than in the wet season (670 ± 145 m, $N = 65$). *Cohen et al*. [2006] report similar low-level jets in eastern Amazonia. The shear generated by the low-level jet is a top-down forcing of the NBL [*R. M. N. dos Santos*, 2005].

Acevedo et al. [2004] estimated NBL depths during two campaigns, July and October 2001 near Santarém, from surface fluxes and local changes in temperature and humidity as measured by tether or captive balloons. For this site not far from the Tapajós River, their estimates of NBL depth were smaller (less than 150 m), comparable to the thickness of the nocturnal fog layer before dawn. They suggest that the radiative flux divergence at the interface between fog and the clear air above leads to a strong temperature inversion. They used budget methods to compare the accumulation of CO_2 in the NBL with eddy correlation estimates of the surface CO_2 flux.

2.5. Local Thermodynamic BL Processes and Land-Surface Feedback

We will shift attention now to the coupling of surface, BL, and atmospheric processes and discuss some of the links between surface evaporation, cloud base, cloud cover, and surface cloud radiative forcing on the daily timescale [*Betts*, 2004; *Betts and Viterbo*, 2005]. For illustration, we again use the ERA-40 reanalysis for the period 1990–2001 averaged over the Rio Madeira Basin. We averaged the hourly model data to give daily means. When we average over the diurnal cycle, we see the balance on the daily timescale between surface processes, downward mixing into the BL, and the effect of falling precipitation evaporating into the BL. In the model system, soil water is a strong control on evaporation as well as BL and cloud processes [*Betts and Viterbo*, 2005]. However, the model does not represent well the Amazonian soils and deep rooting structures, and compared to Figure 4 for the Jaru forest, the model has much less water available for evapotranspiration in the dry season. So instead of soil water storage, we will use the surface evaporative fraction, $EF = \lambda E/(\lambda E + H)$, to represent the range of availability of surface and subsurface water states. EF can also be thought of as the fraction of the surface available energy going into evapotranspiration.

Figure 7 has four plots. Figure 7a links surface evaporative fraction, EF, to near-surface RH and P_{LCL} (the height of the LCL or cloud base) for different daily precipitation rates. A representative set of standard deviations of the daily mean data is shown. Not surprisingly, as EF increases, mean cloud base descends and RH increases; but RH also increases as precipitation increases. This is a highly coupled system.

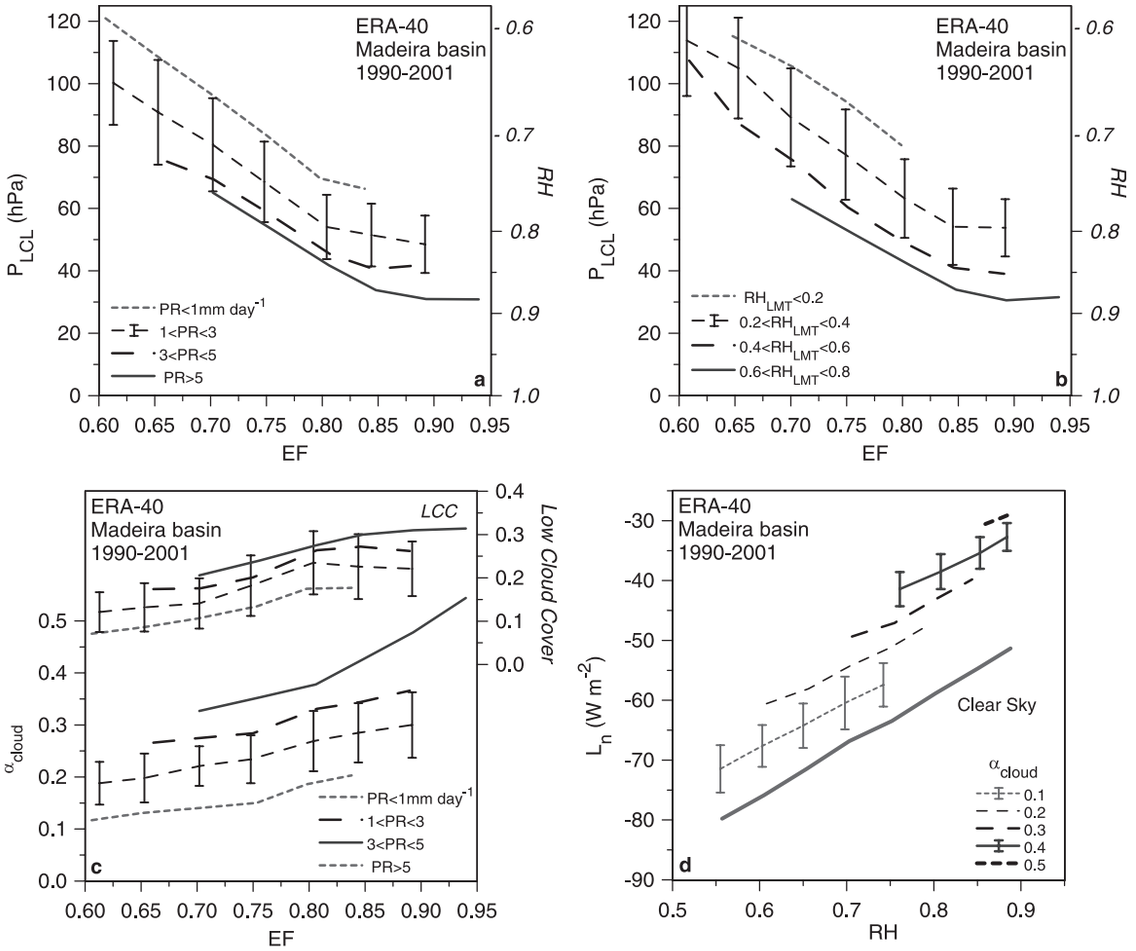

Figure 7. (a) Near-surface P_{LCL} and RH as a function of EF and daily precipitation rate (PR). (b) Same as Figure 7a but for a function of lower middle tropospheric RH. (c) Cloud albedo and low cloud cover as a function of EF and PR. (d) Surface net long-wave flux as a function of RH and cloud albedo.

When the LCL is lower, more precipitation is likely; but the converse is also true: the evaporation of precipitation as it falls through the subcloud layer will lower the LCL.

Now the balance of the subcloud layer depends not only on the surface EF but also on the humidity of the air above the BL, which the BL entrains as it grows deeper during the daytime. Figure 7b is similar to Figure 7a, but the days have been stratified by RH_{LMT}, which is the average daily RH for the lower middle tropospheric (LMT) layer between 500 and 700 hPa (typically above the BL). The RH of the subcloud layer shifts toward a moister state as the lower middle troposphere gets moister. Figures 7a and 7b look rather similar because the RH of the lower middle troposphere and the precipitation are themselves coupled to the midtropospheric vertical motion field on the daily timescale [*Betts and Viterbo*, 2005].

Figure 7c, upper curves, shows that the model low cloud fraction below 700 hPa increases weakly with EF and is coupled to increasing precipitation. A more quantitative measure of the cloud field is the surface short-wave cloud radiative forcing (SWCF), defined as $SW_{dn} - SW_{dn}(clear)$, the reduction in the incoming clear-sky surface downward short-wave flux (SW_{dn}) by the cloud field. From the SWCF, we can define (following *Betts et al*. [2006]) a nondimensional measure, the effective surface cloud albedo, α_{cloud}, as

$$\alpha_{cloud} = -SWCF/SW_{dn}(clear). \quad (1)$$

The lower curves in Figure 7c show that α_{cloud}, related to the short-wave cloud forcing, increases with surface EF and quite strongly with precipitation rate. We used the ERA-40 clear-sky flux to compute α_{cloud} in (1). Since ERA-40 has only a seasonal representation of aerosols, the strong variability in atmospheric aerosol absorption due to local fires (extensive in the dry-to-wet season) will be projected in this analysis onto the cloud forcing and α_{cloud}.

Figure 7d shows the link between the mean surface RH and the surface net long-wave flux, L_n, stratified by α_{cloud}. The lowest curve is the clear-sky L_n: we see that the outgoing net clear-sky flux decreases sharply as the BL gets moister and cloud base lowers. The upward shift of L_n with increasing cloud is a measure of the long-wave cloud forcing on the daily timescale. Note that the standard deviations of the daily data are rather small, typically <5 W m^{-2}. *Betts et al.* [2006] showed that these long-wave relationships in ERA-40 were in close agreement with flux tower measurements over the boreal forest.

Can we evaluate any of these model relationships using data from LBA? Figure 8 shows some similarities and differences between the data (Figures 8b and 8d) from the Rebio Jaru forest site [*von Randow et al.*, 2004] and the nearest grid point in ERA-40 (Figures 8a and 8c). Precipitation at a point is too noisy a field for stratification, and we have few upper air observations during these 4 years of near-surface

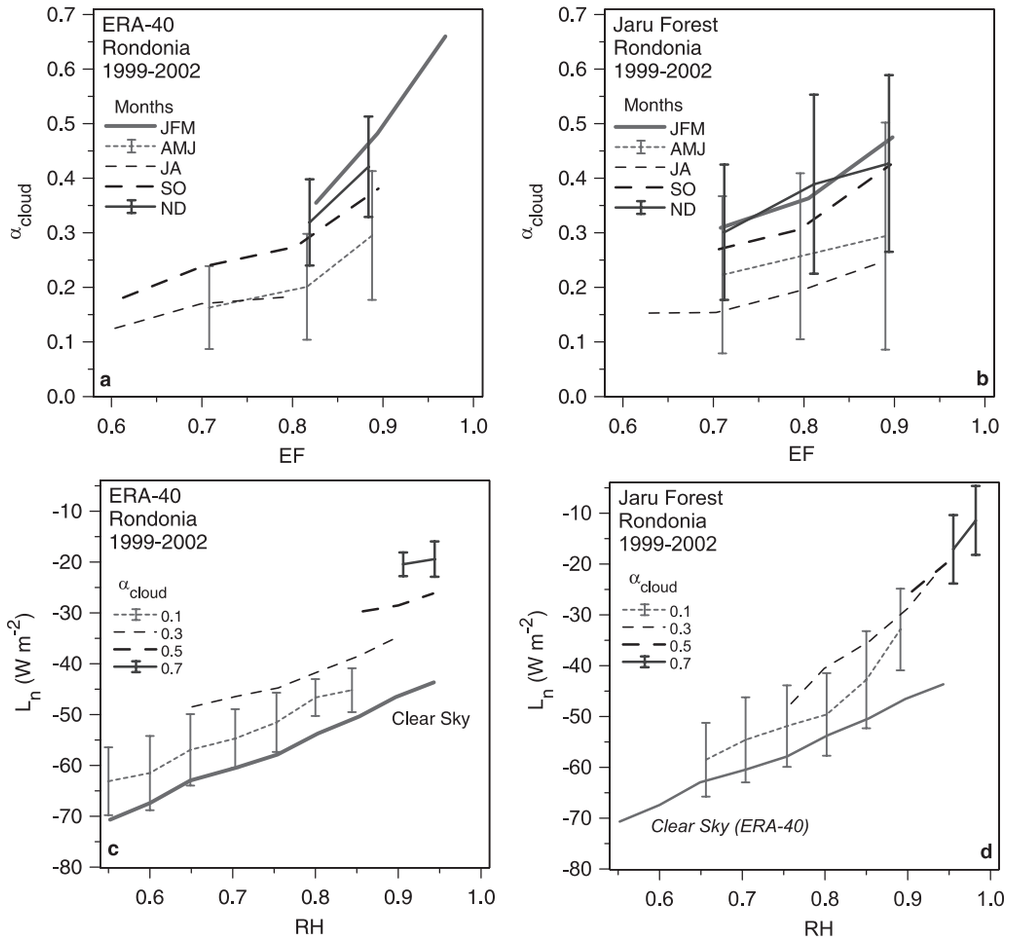

Figure 8. (a and b) Cloud albedo as a function of EF and season for ERA-40 and Jaru forest data. (c and d) Surface net long-wave flux as a function of RH and cloud albedo for ERA-40 and Jaru forest. Abbreviations are JFM, January, February, and March (the wet season); AMJ, April, May, and June; JA, July and August (the dry season); SO, September and October (dry-to-wet transition); and ND, onset of the wet season.

data. So, instead, we used a seasonal stratification, dividing the year into five monthly groups: January, February, and March, the wet season; April, May, and June; July and August, the dry season; September and October, dry-to-wet transition; and the onset of the wet season. Figures 8a and 8b compare the dependence of α_{cloud} on EF. ERA-40 has a larger seasonal range of EF: greater in the wet season and smaller in the dry season than the Jaru forest. However, the lack of energy balance closure in the eddy correlation forest flux measurements, used here as daily means, introduces some uncertainty into the data. *von Randow et al.* [2004] showed that attributing the entire energy imbalance to an underestimate in the evaporation would increase EF. Figure 8a shows for ERA-40 the increase in cloud with surface evaporation and with the seasonal change in the large-scale forcing between dry and wet seasons. Figure 8b shows a similar seasonal change and a weak increase with EF, but the representative error bars shown are significantly larger for the data than the reanalysis.

Figures 8c and 8d show the coupling of surface net longwave, L_n, with near-surface RH and derived α_{cloud}. ERA-40 has a dry bias with respect to the forest site in all seasons (not shown). The reanalysis data are at the lowest model level (about 10 m), and the forest measurements are at 60 m, and this could account for 2% of this bias. ERA-40 has a wider seasonal range of RH. Since ERA-40 has much less soil water storage than is available to the Jaru forest (Figure 4), this leads to lower values of both EF and RH in the dry season in the reanalysis. Figure 8c for a single grid point is similar to Figure 7d for the much larger Madeira Basin. It shows the fall in outgoing L_n with increasing humidity and increasing cloud. Figure 8d, the corresponding plot derived from the forest observations (using the ERA-40 clear-sky flux calculation), is similar, but the range of dependence on cloud is reduced, and the standard deviations are again larger. In general terms, the Amazonian forest with deeper rooting and large soil moisture reserves has a smaller seasonal variation in the surface fluxes than ERA-40. Consequently, the Amazonian surface fluxes and BL are less strongly coupled to the atmospheric forcing than in ERA-40. The forest provides a local climate stability, which is lost with deforestation, when effective soil water storage is reduced.

The daily mean fields and fluxes give a coherent picture of the local land-surface-atmosphere interaction, and from them we can draw inferences about the feedback of land surface memory on the seasonal evolution of the boundary layer and convection. *Fu and Li* [2004] looked at the interannual variability of the onset of the wet season and its links to rainfall in the dry season using 15 years of the ERA-40 data. They found that a longer dry season with less rainfall, and therefore reduced evaporation, led to reduced convective available potential energy (CAPE), greater stability, and a seasonal delay in the initiation of precipitation and the onset of the rainy season. This is fully consistent with Figure 7a, where we see that a lower evaporative fraction and precipitation gives a drier near-surface RH with a corresponding higher cloud base LCL. They suggested that if land use change in Amazonia increased the severity of the dry season, this would also delay the onset of the rainy season. However, local land-surface feedbacks interact with processes of larger scale in determining the circulation. *Li and Fu* [2006] show the impact of cold front intrusions on the wet season onset. *Grimm et al.* [2007] suggest that low spring precipitation leads to low spring soil moisture and high late spring surface temperature in central east Brazil. This induces a topographically enhanced low-level anomalous convergence and cyclonic circulation over southeast Brazil, which enhances the moisture flux from northern and central South America into central east Brazil, setting up favorable conditions for excess rainfall during the peak summer monsoon. This relation is especially strong during El Niño–Southern Oscillation years. Antecedent wet conditions in spring lead to opposite anomalies. They also suggest that the mountains of southeast Brazil may play a role in anchoring the patterns of intraseasonal variability.

3. NATURE OF AMAZONIAN CONVECTION

In the rainy season, convection over Amazonia is sensitive to processes on many time and space scales because the BL is so close to moist neutrality. Unless suppressed by cloud cover, surface evaporation from the forest is generally high, typically around 4 mm d^{-1} [*Shuttleworth*, 1988], and this generates convective instability. *Machado et al.* [2004] used long time series of radiosonde data and the ISCCP satellite data for cloud cover to discuss the climatological aspects of the seasonal and diurnal variability of convection over Amazonia. Equatorial forest sites, Manaus and Belém (Figure 1), have smaller seasonal amplitudes of cloud cover and precipitation than sites within the deforested arc of southern Amazonia (Vilhena) and savanna (Brasília). Equatorial and forest sites show significant seasonal cycles in precipitation and cloud cover, but these are linked to rather small seasonal changes in CAPE. During the rainy season, the differences among the sites are quite small. Greater differences in precipitation, cloud cover, vegetation stress, and thermodynamics appear during the dry season. The strongest thunderstorms occur during the transition dry-to-wet season and at the beginning of the wet season, when atmospheric CAPE is largest for nearly all sites. During the rainy season, the atmosphere is close to the saturated adiabatic lapse rate because of the large area covered by convective cloud

systems. The high cloud fraction, closely associated with the convective clouds, has nearly the same mean diurnal phase for the wet and dry seasons for all regions. A high cloud minimum in the morning (0% and 15% in the dry and wet seasons, respectively) is followed by a rapid increase in the early afternoon, reaching a maximum (20% and 45% in dry and wet seasons, respectively) at the end of the afternoon. The maximum total cloud cover during the wet season is during the night. The majority of the rain events during the wet season occur around 1400 LST in Belém; Manaus has a secondary maximum around 2000 LST, and Brasília also has the majority of rain events at this time [*Machado et al.*, 2004]. The synoptic-scale convective cloud organization, mainly associated with the South Atlantic Convergence Zone (SACZ), and Amazonian squall lines are important features in central Amazonia. The savanna and deforested regions have a larger frequency of thunderstorms, associated with larger CAPE, than the forest sites. Near Belém, sea breeze and river breeze effects influence local convection. In Rondônia during the rainy seasons of 1992 to 1995, *Ferreira da Costa et al.* [1998] found that the time of the maximum rainfall was later (1600 LST) at the forest than at the pasture site (1400 LST).

3.1. Amazonian Convection and the Diurnal Cycle

The daytime convective BL typically goes through a rapid deepening phase, which last several hours until the first cumulus congestus form around 1100 LST [*Pereira et al.*, 2000; *Betts et al.*, 2002a; *Silva Dia*s *et al.*, 2002a]. The cold pools formed by the precipitation-driven downdrafts from these cumulus congestus then start the upscale organization of precipitating convective lines, which subsequently stabilize the BL and troposphere in the afternoon. However, the convective response to small perturbations in stability is rapid, and large-scale forcing can organize propagating squall lines of larger scale and can also force precipitation at night. *Rickenbach* [2004] examines the origins of a secondary nocturnal maximum in cloudiness and precipitation in southwestern Amazonia using satellite, radar, sounding, and profiler observations from the TRMM-LBA and WETAMC field campaigns in early 1999. They found that following locally generated afternoon convection, organized deep convection often contributes to a postmidnight maximum in the rainy area and high cloudiness. Many of these nocturnal convective events can be traced to large-scale squall lines, which propagate westward thousands of kilometers from their origin along the northeast coast of Brazil [*Cohen et al.*, 1995]. Nocturnal stratiform drizzle and cloudiness typically weaken and delay the onset of the following afternoon's convection because they stabilize the atmosphere and leave extensive midlevel clouds, which reduce the morning incoming solar radiation and evaporation [*Betts and Jakob*, 2002b; *Rickenbach*, 2004].

3.2. Modeling the Diurnal Cycle of Convection Over Amazonia

Modeling the diurnal cycle of convection over Amazonia in large-scale models has, however, proved challenging, just because the BL is so close to moist neutrality in the rainy season and responds so rapidly to both large-scale forcing and to radiative feedbacks on the diurnal cycle of the surface fluxes. Global forecast and climate models use convection parameterizations, and these typically produce deep convection soon after sunrise [*Betts and Jakob*, 2002a, 2002b], as soon as the convection scheme "sees" the deep unstable atmosphere, characteristic of the rainy season (Figure 3). Modifications to the convection scheme in the ECMWF model [*Bechtold et al.*, 2004], in which thicker layers are lifted and tested for instability, produced some improvement but only delayed the onset of deep convection a few hours. This appears to be an intrinsic problem because the parameterizations do not handle the development time scale of the highly turbulent shallow convective boundary layer as it grows through the morning hours until the first precipitating congestus form around 1100 LST. These generate the cold pools that organize the subsequent deep convection [*Tompkins*, 2001], a process that also takes a few hours. Models that resolve the explicit development of deep convection have proved more successful in realistically simulating the diurnal cycle of precipitation [*Silva Dias et al.*, 2002b]. *Ramos da Silva and Avissar* [2006] using a 1-km resolution model for Rondônia show that the diurnal cycle of domain-averaged accumulated rainfall can be properly simulated with suitable initial profiles of atmospheric relative humidity and soil moisture. *Khairoutdinov and Randall* [2006] using a very high resolution model (with a 100-m horizontal grid) and specified surface fluxes have successfully simulated the shallow to deep transition for a sample day from the TRMM-LBA experiment (23 February 1999). They explicitly show the role of cold pools from the first precipitating congestus in organizing the development of deep convection. However, it is fair to say that the successful simulation of all the interacting scales in global models has not yet been accomplished.

3.3. Synoptic Links: Mesoscale Analyses of Amazonian Convection

Prior to the LBA field campaigns, *Cohen et al.* [1989] established the climatology of squall line systems originating on the north coast of Brazil. They found the largest fre-

quency between April and August. ABLE 2B [*Harriss et al.*, 1990], which took place from 13 April to 13 May 1987, further characterized the environmental conditions associated with Amazonian convection and squall lines [*Greco et al.*, 1990; *Garstang et al.*, 1994; *Cohen et al.*, 1995]. The initiation of squall lines near the Brazilian northeast coast involves an interaction of easterly waves, sea breeze circulations, and the continental heat source [*Cohen et al.*, 1995]. Once initiated in this favorable synoptic environment with a lower tropospheric easterly jet, squall lines can propagate in a quasi-steady fashion toward the southwest, covering 1000 km in 24 hours (a propagation speed of 12.8 m s^{-1}). Similar formation and westward propagation also occur in the summer rainy season (July–August) over Venezuela if there is a similar easterly flow [*Betts et al.*, 1976; *Fernandez*, 1980], although system lifetimes are typically only a few hours.

During the South American summer, an upper tropospheric anticyclonic circulation known as the Bolivian High is followed in the east by a trough, which extends over the western Atlantic Ocean, known as the northeast Brazilian trough [*Kousky and Gan*, 1981; *Albrecht and Silva Dias*, 2005]. At low levels, a continental heat low develops over Gran Chaco in Argentina. This low-level atmospheric circulation pattern has a northwesterly flow along the eastern Andes in the tropics and subtropics and a predominant east-northeasterly flow over the Amazon Basin, accompanied by intense convective activity and precipitation. *Kousky* [1979] observed that the slow moving cold fronts and subtropical upper tropospheric cyclonic vortices play an important role in characterizing the precipitation over Brazil. These quasi-stationary fronts are referred to as the South Atlantic Convergence Zone [*Nobre*, 1988], and they are recognized as one of the main features of the wet season [*Silva Dias and Marengo*, 1999]. *Seluchi and Marengo* [2000] found that meridional transport of air between the tropics and midlatitudes in South America is the most intense in the entire Southern Hemisphere and is a function of the position of the SACZ. As previous studies suggested that the characterization of the low-level jets in South America is due to these baroclinic systems, many authors have studied the connection between the SACZ and convection over the Amazon Basin, using data collected during the LBA WETAMC and TRMM field experiments in Rondônia [*Carvalho et al.*, 2002; *Halverson et al.*, 2002; *Herdies et al.*, 2002; *Pereira Filho et al.*, 2002; *Rickenbach et al.*, 2002; *Silva Dias et al.*, 2002a; *Tokay et al.*, 2002].

Wet season (January and February) precipitation over the Amazon Basin is clearly linked to the synoptic pattern over South America. Two distinct regimes of lower tropospheric winds (westerlies and easterlies) were observed in Rondônia [*Herdies et al.*, 2002; *Rickenbach et al.*, 2002] during the WETAMC and TRMM components of LBA [*Silva Dias et al.*, 2002a]. The westerly (easterly) winds were associated with strong (weak) convective activity over the SACZ. Variations in the strength of the SACZ regime is in turn associated with the intraseasonal oscillation [*Carvalho et al.*, 2002; *Albrecht and Silva Dias*, 2005]. A stronger SACZ regime is more efficient in transporting tropical moisture from the Amazon Basin into the extratropics. Observations from surface-based radar [*Rickenbach et al.*, 2002] suggested that mesoscale convective systems in the strong SACZ regime were significantly larger in areal coverage, with weaker rainfall intensity and weaker vertical development of the convective cells. The diurnal variation of rain intensity and rain areal coverage generally showed afternoon maxima for both regimes but with important differences, suggesting more explosive convective cell growth in the non-SACZ regime and the dominance of nocturnal stratiform rain processes in the SACZ regime. Individual case studies support this picture of propagating squall line systems in the low-level easterly flow regime with stronger updrafts and more precipitation ice in the middle and upper troposphere [*Cifelli et al.*, 2002; *Pereira Filho et al.*, 2002] and greater electrification [*Halverson et al.*, 2002; *Peterson et al.*, 2002]. The westerly regimes are characterized by reduced CAPE and weaker stratiform rain systems with convective elements embedded in a moister environment [*Cifelli et al.*, 2002; *Halverson et al.*, 2002].

Petersen et al. [2006] reformulated this classification of flow regimes in terms of perturbations to the cross-equatorial flow. They showed, using TRMM lightning and precipitation data from four wet seasons, that it is the southeasterly cross-equatorial flow that has the greatest rain intensities, thermodynamic instability, and electrification. In contrast, the regime associated with a northerly low-level cross-equatorial flow (which gives low-level westerly shear) has more stratiform rain in a moister troposphere but has less convective instability and electrification.

3.4. Aerosols, Smoke, and Convective Transports

Aerosols, coming from natural sources and fires, play a key role over Amazonia, both radiatively, impacting the surface fluxes and BL stability, and in the nucleation of moist convection. Aerosol particle number size distributions and hygroscopic properties were measured [*Rissler at al*., 2006] at a pasture site in Rondônia. The measurements were performed from 11 September to 14 November 2002 as part of LBA SMOCC and cover the latter part of the dry season (with heavy biomass burning), a transition period, and the onset of the wet season. These show the diurnal cycle of the aerosol size distributions and hygroscopic properties, coupled to the diurnal evolution of the boundary layer, decreasing

during the morning with vertical mixing and increasing in the afternoon with peak fire activity (in the latter part of the dry season). The radiative impact of aerosols is to redistribute heat within the atmospheric BL. During the dry season, aerosol absorption produces a thermal stabilization of the atmosphere, which inhibits convection [*Freitas et al.*, 2007; *L. A. R. dos Santos*, 2005] by both the reduction in the surface net radiative flux and the warming of the upper aerosol layer.

Aerosol concentrations significantly alter cloud microphysics. *Andreae et al.* [2004] suggest that the heavy smoke observed from forest fires in the Amazon Basin reduces cloud droplet size and so delays the onset of precipitation from 1.5 km above cloud base in pristine clouds to more than 5 km in polluted clouds and more than 7 km in pyroclouds above fires. Suppression of low-level rainout and aerosol washout allows the transport of water and smoke to upper levels, where the clouds appear "smoking" as they detrain much of the pollution. Elevating the onset of precipitation means the latent heat of freezing is released at higher levels, causing intense thunderstorms, large hail, and greater likelihood for overshooting cloud tops into the stratosphere. Pollutants and water vapor detrained in the lower stratosphere may have profound radiative impacts on the climate system.

3.5. Impact of Microphysical and Electrical Differences on Convection

Over Amazonia, the traditional distinction between "maritime" clouds containing small concentrations (about 50 to 100 cm^{-3}) of large droplets and "continental" clouds containing tenfold-larger concentrations of smaller droplets is blurred. Maritime clouds precipitate easily by warm processes, whereas coalescence is often suppressed in continental clouds, which often have to grow vertically to supercooled levels to precipitate by cold processes involving the ice phase. This distinction between convective clouds remained a microphysical one until the observations of lightning from space revealed a dramatic contrast between the lightning over land and ocean [*Orville and Henderson*, 1986]. The differences in updraft strength above land and ocean surfaces, related to the greater CAPE over land [*Rutledge et al.*, 1992; *Williams et al.*, 1992], were then identified as another cause for differences in the cloud microphysical and electrical properties. *Williams et al.* [2002] examined four distinct meteorological regimes in Amazonia to try to separate the roles of boundary layer aerosol and CAPE in determining continental cloud structure and electrification. The "green ocean" westerly regime of the Amazonian wet season is a distinctly maritime-like regime with minimum aerosol concentration, minimum CAPE (of the order of 1000 J kg^{-1}), and little if any lightning. During the wet season easterly wind regimes, aerosol concentration, CAPE, and lightning yield per unit of rainfall are all larger, so it is not possible to determine whether greater aerosol or CAPE is responsible for greater electrification. The highly polluted aerosol-rich October, when biomass burning is at a peak [*Fuzzi et al.*, 2007] at the end of the dry season in Rondônia, is characterized by large values of CAPE and high electrical activity. Evidence for a substantial role for aerosol in suppressing warm rain coalescence was seen in this most highly polluted period. However, the lack of distinction in the electrical parameters (peak flash rate and lightning yield per unit rainfall) between aerosol-rich October and aerosol-poor November in the premonsoon regime again casts doubt on a primary role for aerosol in enhancing cloud electrification.

3.6. Coupling of Ozone Transport to Deep Convection

Vertical transports by moist convection are the primary process for mixing in the tropical atmosphere. Atmospheric constituents are mixed throughout the convective BL during the period of morning growth, and with the onset of deep convection, convective updrafts and downdrafts, driven by condensation and evaporation, overturn the whole troposphere. Near-surface measurements of equivalent potential temperature and ozone at night, when background levels of ozone are low, clearly show that convective downdrafts rapidly transport air with higher ozone and lower equivalent potential temperature down to the surface from around 800 hPa [*Betts et al.*, 2002b]. This downward transport of ozone may play a significant role in the photochemistry of the atmosphere boundary layer and increase the surface deposition of ozone. The upward transport of low-ozone air by deep convection in turn affects the photochemistry of the upper troposphere and gives insight into the convective mass transports [*Kley et al.*, 1997, 2007]

3.7. Forest Breeze and River Breeze Circulations

Given the instability of the Amazonian atmosphere, differences in the surface forcing can affect the convective organization. The challenge of understanding and modeling this over Amazonia has been the subject of several papers. *Silva Dias and Regnier* [1996] addressed the modeling of mesoscale circulations driven by a deforested region in Rondônia using a mesoscale model. *Souza et al.* [2000] proposed a simple theory for how temperature differences forced by surface heterogeneities can force mesoscale circulations and applied it to the forest-pasture differences seen in RBLE 3 data collected in the dry season in Rondônia. *Silva Dias et al.* [2002b] examined the impact of topography and defor-

estation on the development of organized precipitating lines in Rondônia using data from dual Doppler radar analysis, radiosondes, and surface and boundary layer observations. They complemented the observational study with a series of regional high-resolution model simulations at 2-km resolution over a 300 km × 300 km area initialized by a morning radiosonde profile. They concluded that during a period of very weak large-scale forcing, topography and deforestation played a significant role, although the discrete propagation of individual cells and their coupling with upper atmosphere circulations were responsible for the development of multiple lines.

River breeze circulations also play an important role in organizing Amazonian convection [*de Oliveira and Fitzjarrald*, 1993; *Silva Dias et al.*, 2004; *Lu et al.*, 2005]. The Santarém Mesoscale Campaign was conducted in August 2001 close to two major rivers of the Amazon Basin, the Tapajós and the Amazon. The observations indicate that during weak trade wind episodes, the Tapajós River breeze actually induces a westerly flow at the eastern margin with an associated line of shallow cumulus. With strong trade winds, the river breeze still slows the easterly flow over the river and organizes cloud lines east of the river. The atmospheric circulation induced by the river has been interpreted with the help of a high-resolution numerical simulation. A single cell forms during late morning over the Rio Tapajós, and it evolves in the afternoon with ascending motion in the eastern margin and a descending branch in the western margin, which suppresses cloud formation. During the night, convergence is seen along the center of the Tapajós. The atmospheric CO_2 concentration variations were simulated using the Colorado State University Regional Atmospheric Modeling System with four nested grids that included a 1-km finest grid centered on the Tapajós National Forest [*Lu et al.*, 2005]. The results also suggested that the topography, the differences in roughness length between water and land, the "T" shape juxtaposition of Amazon and Tapajós rivers, and the resulting horizontal and vertical wind shears all facilitated the generation of local mesoscale circulations. Thus the particular geometry of the rivers with respect to the trade winds has implications for the generalization of the surface measurements of turbulent fluxes of heat, moisture, and CO_2 in the Tapajós region.

4. CONCLUSIONS

The field experiments in Amazonia have given us a rich database of information on the BL in different regions and seasons over both forest and pasture, which show the interaction of many processes. The surface radiative fluxes are modulated by the solar seasonal cycle and the daily and seasonal variation in cloud cover and atmospheric aerosols. The partition of the surface net radiation into sensible and latent heat fluxes depends largely on the availability of water for evapotranspiration. Over the forest, where rooting is deep and the soil moisture reservoir is large, the annual cycle of evapotranspiration is small, even where there is a long dry season (as in Rondônia in SW Amazonia). Large daytime surface evaporation generates moist convective instability and a strong diurnal cycle of convection, which is sensitive to dynamic forcing on larger scales. When forcing is weak, the unstable convective BL of shallow cumulus grows rapidly until about 1100 LST, when the BL is deep enough that the first cumulus congestus form and precipitate. Evaporating precipitation drives downdrafts, and the cold outflow boundaries start the self-organization of the convection into lines of precipitating cumulonimbus. When dynamic forcing is strong, precipitation and cloudiness may peak at night. The nighttime BL over the forest typically saturates and forms a layer of fog, some 150 m deep with strong radiative cooling at the top.

The seasonal cycle is controlled by processes of much larger scale. In August, large-scale subsidence dominates over Rondônia, drying the troposphere and suppressing the convective BL sufficiently that precipitation is greatly reduced. Over deforested pastures, where access to deep soil water is greatly reduced, EF drops substantially in the dry season, and afternoon cloud base may rise to 2000 m with reduced shallow cumulus cloud cover. The diurnal range of temperature doubles as the surface net long-wave cooling also doubles. The dry-to-wet transition season is marked by the largest atmospheric CAPE, high levels of smoke aerosols from widespread fires, the most energetic deep convection with the highest tops, and the greatest lightning flash rates. The primary vertical transport is by deep convection, exchanging gases, aerosols, and smoke between the BL and the upper troposphere.

In addition to self-organization on outflow boundaries, mesoscale patterns of convection are organized by heterogeneities in topography or surface heat fluxes, associated with different vegetation and soil water availability. The large Amazonian rivers exert their influence on the low-level flow. The shift in lower tropospheric wind patterns over Rondônia from northeast to northwest, associated with an increase in the intensity of the SACZ, alters the convective organization structure and propagation as they change both the vertical shear and the BL aerosols feeding into clouds. In the low-level easterly flow regime, propagating squall line systems predominate, with stronger updrafts and more precipitation ice in the middle and upper troposphere and greater electrification. The westerly regimes are characterized by reduced CAPE and weaker stratiform rain systems with convective

elements embedded in a moister environment. Squall lines of still larger scale originate from the northeast coast, and their influence propagates for days, organizing convection and particularly driving precipitation at night.

Stepping back, we have made considerable progress in describing and understanding the complex interactions between the continental-scale meteorology and climate of South America and more local processes: such as the coupling of biosphere, aerosols, and microphysics; clouds, rain and mesoscale processes over the diurnal cycle; and the vertical coupling between the surface, boundary layer, cloud radiative forcing, and troposphere. From an observational perspective, continuous monitoring of BL depth using sodars or lidars could substantially help further analyses. A few regions have not yet been studied, such as NW Amazonia, which has an intact forest and no dry season, and the areas of savannah with tropical forest in Roraima State in north Amazonia. Advective processes at the transitions between forest and deforested areas need more investigation, specifically in their energy, water, and carbon budgets; high-resolution modeling could be useful for this.

Yet substantial modeling problems remain because our computational capability is still insufficient to represent the whole range of scales from the microphysical to the global and the development of satisfactory parameterizations for the smaller scales has been slow. Amazonia is a particularly challenging modeling environment because during the rainy season the atmosphere is so close to saturation and hence so unstable to moist processes on a range of scales. As a result, forecast and climate models differ in their land-surface-BL-cloud coupling, and many still have errors in the diurnal cycle. Consequently, the careful evaluation of models against the rich database of Amazonian observations still provides a critical path forward.

Acknowledgments. Alan Betts acknowledges support from NSF under grant ATM0529797 and from NASA under NEWS grant NNG05GQ88A. Maria Assunção F. da Silva Dias, Gilberto Fisch, and Otavio Acevedo acknowledge the support of Conselho Nacional de Desenvolvimento Científico e Tecnológico through their research grant (PQ). FAPESP and MCT/Milênio also funded part of the research.

REFERENCES

Acevedo, O. C., O. L. L. Moraes, R. da Silva, D. R. Fitzjarrald, R. K. Sakai, R. M. Staebler, and M. J. Czikowsky (2004), Inferring nocturnal surface fluxes from vertical profiles of scalars in an Amazon pasture, *Global Change Biol.*, *10*, 1–9, doi:10.1111/j.1529-8817.2003.00755.x.

Albrecht, R. I., and M. A. F. Silva Dias (2005), Microphysical evidence of the transition between predominant convective/stratiform rainfall associated with the intraseasonal oscillation in the southwest Amazon, *Acta Amazonica*, *35*(2), 175–184.

Andreae, M. O., D. Rosenfeld, P. Artaxo, A. A. Costa, G. P. Frank, K. M. Longo, and M. A. F. Silva-Dias (2004), Smoking rain clouds over the Amazon, *Science*, *303*, 1337–1342.

Bechtold, P., J.-P. Chaboureau, A. Beljaars, A. K. Betts, M. Miller, M. Köhler, M. Miller, and J.-L. Redelsperger (2004), The simulation of the diurnal cycle of convective precipitation over land in a global model, *Q. J. R. Meteorol. Soc*., *130*, 3119–3137.

Betts, A. K. (1976), The thermodynamic transformation of the tropical subcloud layer by precipitation and downdrafts, *J. Atmos. Sci*., *33*, 1008–1020.

Betts, A. K. (2003), Diurnal cycle, in *Encyclopedia of Atmospheric Sciences*, edited by J. R. Holton, J. Pyle, and J. A. Curry, pp. 640–643, Academic, London.

Betts, A. K. (2004), Understanding hydrometeorology using global models, *Bull. Am. Meteorol. Soc*., *85*, 1673–1688.

Betts, A. K. (2006), Radiative scaling of the nocturnal boundary layer and the diurnal temperature range, *J. Geophys. Res.*, *111*, D07105, doi:10.1029/2005JD006560.

Betts, A. K., and C. Jakob (2002a), Evaluation of the diurnal cycle of precipitation, surface thermodynamics, and surface fluxes in the ECMWF model using LBA data, *J. Geophys. Res.*, *107*(D20), 8045, doi:10.1029/2001JD000427.

Betts, A. K., and C. Jakob (2002b), Study of diurnal cycle of convective precipitation over Amazonia using a single column model, *J. Geophys. Res.*, *107*(D23), 4732, doi:10.1029/2002JD002264.

Betts, A. K., and P. Viterbo (2005), Land-surface, boundary layer, and cloud-field coupling over the southwestern Amazon in ERA-40, *J. Geophys. Res.*, *110*, D14108, doi:10.1029/2004JD005702.

Betts, A. K., R. W. Grover, and M. W. Moncrieff (1976), Structure and motion of tropical squall lines over Venezuela, *Q. J. R. Meteorol. Soc.*, *102*, 395–404.

Betts, A. K., J. D. Fuentes, M. Garstang, and J. H. Ball (2002a), Surface diurnal cycle and boundary layer structure over Rondônia during the rainy season, *J. Geophys. Res.*, *107*(D20), 8065, doi:10.1029/2001JD000356.

Betts, A. K., L. V. Gatti, A. M. Cordova, M. A. F. Silva Dias, and J. D. Fuentes (2002b), Transport of ozone to the surface by convective downdrafts at night, *J. Geophys. Res.*, *107*(D20), 8046, doi:10.1029/2000JD000158.

Betts, A. K., J. H. Ball, and J. Fuentes (2002c), Calibration and correction of LBA/TRMM Abracos pasture site merged dataset, ftp://daac.ornl.gov/data/lba/physical_climate/Betts, Oak Ridge Natl. Lab., Oak Ridge, Tenn.

Betts, A. K., J. Ball, A. Barr, T. A. Black, J. H. McCaughey, and P. Viterbo (2006), Assessing land-surface-atmosphere coupling in the ERA-40 reanalysis with boreal forest data, *Agric. For. Meteorol.*, *140*, 355–382, doi:10.1016/j.agrformet.2006.08.009.

Betts, A. K., R. Desjardins, and D. Worth (2007), Impact of agriculture, forest and cloud feedback on the surface energy balance in BOREAS, *Agric. For. Meteorol.*, *142*, 156–169, doi:10.1016/j.agrformet.2006.08.020.

Carvalho, L. M. V., C. Jones, and M. A. F. Silva Dias (2002), Intraseasonal large-scale circulations and mesoscale convective activ-

ity in tropical South America during the TRMM-LBA campaign, *J. Geophys. Res.*, *107*(D20), 8042, doi:10.1029/2001JD000745.

Cifelli, R., W. A. Petersen, L. D. Carey, S. A. Rutledge, and M. A. F. da Silva Dias (2002), Radar observations of the kinematic, microphysical, and precipitation characteristics of two MCSs in TRMM LBA, *J. Geophys. Res.*, *107*(D20), 8077, doi:10.1029/2000JD000264.

Cohen, J., L. Sa, D. Nogueira, and A. Gandu (2006), High resolution simulation the eastern Amazonia, *87*(36), Jt. Assem. Suppl., Abstract IN33A-06.

Cohen, J. C. P., M. A. F. Silva Dias, and C. A. Nobre (1989), Aspectos climatologico das linhas de instabilidade na Amazonia, *Climanalise Bol. Monit. Anal. Clim.*, *4*, 34–40.

Cohen, J. C. P., M. A. F. Silva Dias, and C. A. Nobre (1995), Environmental conditions associated with Amazonian squall lines: A case study, *Mon. Weather Rev.*, *123*, 3163–3174.

Culf, A. D., J. L. Esteves, A. de O. Marques Filho, and H. R. da Rocha (1996), Radiation, temperature and humidity over forest and pasture in Amazonia, in *Amazonian Deforestation and Climate*, edited by J. H. C. Gash et al., pp. 175–191, John Wiley, New York.

da Rocha, H. R., A. O. Manzi, and J. Shuttleworth (2009), Evapotranspiration, *Geophys. Monogr. Ser.*, doi:10.1029/2008GM000744, this volume.

de Oliveira, A. P., and D. R. Fitzjarrald (1993), The Amazon River breeze and the local boundary layer. 1. Observations, *Bound Layer Meteorol.*, *63*, 141–162.

dos Santos, L. A. R. (2005), Análise e caracterização da camada limite convectiva em área de pastagem, durante o período de transição entre a estação seca e chuvosa na Amazônia (experimento RACCI-LBA/Rondônia), *INPE-14049-TDI/1064*, 118 pp., Inst. Nac. de Pesqui. Espaciais, São José dos Campos, Brazil.

dos Santos, R. M. N. (2005), Study of the nocturnal boundary layer in Amazonia (in Portuguese), Ph.D. thesis, Inst. Nac. de Pesqui. Espaciais, São José dos Campos, Brazil.

Fernandez, W. (1980), Environmental conditions and structure of some types of convective mesoscales observed over Venezuela, *Arch. Meteorol. Geophys. Bioklimatol.*, *Ser. A*, *31*, 71–89.

Ferreira da Costa, R., J. R. P. Feitosa, G. Fisch, S. S. de Souza, and C. A. Nobre (1998), Variabilidade diária da precipitação em regiões de floresta e pastagem na Amazônia, *Acta Amazonica*, *28*, 395–408.

Fisch, G., J. Tota, L. A. T. Machado, M. A. F. Silva Dias, R. F. da F. Lyra, C. A. Nobre, A. J. Dolman, and J. H. C. Gash (2004), The convective boundary layer over pasture and forest in Amazonia, *Theor. Appl. Climatol.*, *78*, 47–59, doi:10.1007/s00704-004-0043-x.

Fisch, G., I. F. Vendrame, and P. C. de M. Hanaoka (2007), Variabilidade espacial da chuva durante o experimento LBA/TRMM 1999 na Amazônia, *Acta Amazonica*, *37*(4), 583–590.

Fisch, H. R., A. D. Culf, and C. A. Nobre (1996), Modeling convective boundary layer growth in Rondônia, in *Amazonian Deforestation and Climate*, edited by J. H. C. Gash et al., pp. 425–435, John Wiley, New York.

Freitas, S. R., et al. (2007), The Coupled Aerosol and Tracer Transport model to the Brazilian developments on the Regional Atmospheric Modeling System (CATT-BRAMS). Part 1: Model description and evaluation, *Atmos. Chem. Phys. Discuss.*, *7*, 8525–8569.

Fu, R., and W. Li (2004), The influence of the land-surface on the transition from dry to wet season in Amazonia, *Theor. Appl. Climatol.*, *78*, 97–110.

Fuzzi, S., et al. (2007), Overview of the inorganic and organic composition of size-segregated aerosol in Rondônia, Brazil, from the biomass-burning period to the onset of the wet season, *J. Geophys. Res.*, *112*, D01201, doi:10.1029/2005JD006741.

Galvão, J. A. da C., and G. Fisch (2000), Balanço de energia em área de floresta e pastagem na Amazônia (Ji-Paraná, RO), *Rev. Bras. Meteorol.*, *15*, 25–37.

Garstang, M., H. L. Massie, J. Halverson, S. Greco, and J. Scala (1994), Amazon coastal squall lines. Part 1: Structure and kinematics, *Mon. Weather Rev.*, *122*, 608–622.

Greco, S., R. Swap, M. Garstang, S. Ulanski, M. Shipman, R. C. Harriss, R. Talbot, M. O. Andreae, and P. Artaxo (1990), Rainfall and surface kinematic conditions over central Amazonia during ABLE 2B, *J. Geophys. Res.*, *95*, 17,001–17,014.

Grimm, A. M., J. S. Pal, and F. Giorgi (2007), Connection between spring conditions and peak summer monsoon rainfall in South America: Role of soil moisture, surface temperature, and topography in eastern Brazil, *J. Clim.*, *20*, 5929–5945.

Halverson, J. B., T. M. Rickenbach, B. Roy, H. Pierce, and E. Williams (2002), Environmental characteristics of convective systems during TRMM-LBA, *Mon. Weather Rev.*, *130*, 1493–1509.

Harriss, R. C., et al. (1990), The Amazon Boundary Layer Experiment: Wet season 1987, *J. Geophys. Res.*, *95*, 16,721–16,736.

Hasler, N., and R. Avissar (2007), What controls evapotranspiration in the Amazon Basin?, *J. Hydrometeorol.*, *8*, 380–395.

Herdies, D. L., A. da Silva, M. A. F. Silva Dias, and R. Nieto Ferreira (2002), Moisture budget of the bimodal pattern of the summer circulation over South America, *J. Geophys. Res.*, *107*(D20), 8075, doi:10.1029/2001JD000997.

Hodnett, M. G., M. D. Oyama, J. Tomasella, and A. de O. Marques Filho (1996), Comparisons of long-term soil water storage behaviour under pasture and forest in three areas of Amazonia, in *Amazonian Deforestation and Climate*, edited by J. H. C. Gash et al., pp. 57–78, John Wiley, New York.

Horel, J. H., A. N. Hahmann, and J. E. Geisler (1989), An investigation of the annual cycle of convective activity over the tropical America, *J. Clim.*, *2*, 1388–1403.

Khairoutdinov, M., and D. Randall (2006), High-resolution simulation of shallow-to-deep convection transition over land, *J. Atmos. Sci.*, *63*, 3421–3436.

Kley, D., H. G. J. Smit, H. Vömel, H. Grassl, V. Ramanathan, P. J. Crutzen, S. Williams, J. Meywerk, and S. J. Oltmans (1997), Tropospheric water vapour and ozone cross sections in a zonal plane over the central equatorial Pacific, *Q. J. R. Meteorol. Soc.*, *123*, 2009–2040.

Kley, D., H. G. J. Smit, S. Nawrath, Z. Luo, P. Nedelec, and R. H. Johnson (2007), Tropical Atlantic convection as revealed by ozone and relative humidity measurements, *J. Geophys. Res.*, *112*, D23109, doi:10.1029/2007JD008599.

Kousky, V. E. (1979), Frontal influences on northeast Brazil, *Mon. Weather Rev.*, *107*, 1140–1153.

Kousky, V. E., and M. A. Gan (1981), Upper tropospheric cyclonic vortices in the tropical South Atlantic, *Tellus*, *33*(6), 538–551.

Li, W., and R. Fu (2006), Influence of cold air intrusions on the wet season onset over Amazonia, *J. Clim.*, *19*, 257–275.

Lu, L., A. S. Denning, M. A. da Silva-Dias, P. da Silva-Dias, M. Longo, S. R. Freitas, and S. Saatchi (2005), Mesoscale circulations and atmospheric CO_2 variations in the Tapajós Region, Pará, Brazil, *J. Geophys. Res.*, *110*, D21102, doi:10.1029/2004JD005757.

Machado, L. A. T., H. Laurent, N. Dessay, and I. Miranda (2004), Seasonal and diurnal variability of convection over the Amazonia: A comparison of different vegetation types and large scale forcing, *Theor. Appl. Climatol.*, *78*, 61–77.

Martin, C. L., D. Fitzjarrald, M. Garstang, A. P. Oliveira, S. Greco, and E. Browell (1988), Structure and growth of the mixing layer over the Amazonian rain forest, *J. Geophys. Res.*, *93*, 1361–1375.

Negrón Juárez, R. I., M. G. Hodnett, R. Fu, M. L. Goulden, and C. von Randow (2007), Control of dry season evapotranspiration over the Amazonian forest as inferred from observations at a southern Amazon forest site, *J. Clim.*, *20*, 2827–2839.

Nobre, C. (1988), Ainda sobre a Zona de Convergência do Atlântico Sul: A importância do Oceano Atlântico, *Climanálise*, *3*(4), 30–33.

Nobre, C. A., G. Fisch, H. R. da Rocha, R. F. F. Lyra, E. P. da Rocha, A. C. L. da Costa, and V. N. Ubarana (1996), Observations of the atmospheric boundary layer in Rondônia, in *Amazonian Deforestation and Climate*, edited by J. H. C. Gash et al., pp. 413–424, John Wiley, New York.

Nobre, C. A., G. O. Obregón, J. A. Marengo, R. Fu, and G. Poveda (2009), Characteristics of Amazonian climate: Main features, *Geophys. Monogr. Ser.*, doi:10.1029/2008GM000720, this volume.

Oliveira, P. J., and G. Fisch (2000), Efeito da turbulência na camada limite atmosférica em áreas de floresta e pastagem na Amazônia, *Acta Amazonica*, *15*, 39–44.

Orville, R. E., and R. W. Henderson (1986), Global distribution of midnight lightning: December 1977 to August 1978, *Mon. Weather Rev.*, *114*, 2640–2653.

Pereira, L. G. P., M. A. F. Silva Dias, A. J. Pereira Filho, and P. T. Matsuo (2000), Timing of convection initiation during the WETAMC-LBA, paper presented at First LBA Scientific Conference, Ministry of Sci. and Technol., Belém, Brazil.

Pereira Filho, A. J., M. A. F. Silva Dias, R. I. Albrecht, L. G. P. Pereira, A. W. Gandu, O. Massambani, A. Tokay, and S. Rutledge (2002), Multisensor analysis of a squall line in the Amazon region, *J. Geophys. Res.*, *107*(D20), 8084, doi:10.1029/2000JD000305.

Petersen, W. A., S. W. Nesbitt, R. J. Blakeslee, R. Cifelli, P. Hein, and S. A. Rutledge (2002), TRMM observations of intraseasonal variability in convective regimes over the Amazon, *J. Clim.*, *15*, 1278–1294.

Petersen, W. A., R. Fu, M. Chen, and R. Blakeslee (2006), Intraseasonal forcing of convection and lightning activity in the southern Amazon as a function of cross-equatorial flow, *J. Clim.*, *19*, 3180–3196.

Ramos da Silva, R., and R. Avissar (2006), The hydrometeorology of a deforested region of the Amazon Basin, *J. Hydrometeorol.*, *7*, 1028–1042.

Rickenbach, T. M. (2004), Nocturnal cloud systems and the diurnal variation of clouds and rainfall in southwestern Amazonia, *Mon. Weather Rev.*, *132*, 1201–1219.

Rickenbach, T. M., R. N. Ferreira, J. B. Halverson, D. L. Herdies, and M. A. F. Silva Dias (2002), Modulation of convection in the southwestern Amazon Basin by extratropical stationary fronts, *J. Geophys. Res.*, *107*(D20), 8040, doi:10.1029/2000JD000263.

Rissler, J., A. Vestin, E. Swietlicki, G. Fisch, J. Zhou, P. Artaxo, and M. O. Andreae (2006), Size distribution and hygroscopic properties of aerosol particles from dry-season biomass burning in Amazonia, *Atmos. Chem. Phys.*, *6*, 471–491.

Rutledge, S. A., E. R. Williams, and T. D. Keenan (1992), The Down Under Doppler and Electricity Experiment (DUNDEE): Overview and preliminary results, *Bull. Am. Meteorol. Soc.*, *73*, 3–16.

Seluchi, M. E., and J. A. Marengo (2000), Tropical-midlatitude exchange of air masses during summer and winter in South America: Climatic aspects and examples of intense events, *Int. J. Climatol.*, *20*, 1167–1190.

Shuttleworth, W. J. (1988), Evaporation from Amazonian rainforest, *Proc. R. Soc. London*, *Ser. B, 233*, 321–346.

Silva Dias, M. A. F., and P. Regnier (1996), Simulation of mesoscale circulations in a deforested area of Rondônia in the dry season, in *Amazonian Deforestation and Climate,* edited by J. H. C. Gash et al., pp. 531–547, John Wiley, New York.

Silva Dias, M. A. F., et al. (2002a), Cloud and rain processes in a biosphere-atmosphere interaction context in the Amazon Region, *J. Geophys. Res.*, *107*(D20), 8072, doi:10.1029/2001JD000335.

Silva Dias, M. A. F., et al. (2002b), A case study of convective organization into precipitating lines in the southwest Amazon during the WETAMC and TRMM-LBA, *J. Geophys. Res.*, *107*(D20), 8078, doi:10.1029/2001JD000375.

Silva Dias, M. A. F., P. L. Silva Dias, M. Longo, D. R. Fitzjarrald, and A. S. Denning (2004), River breeze circulation in eastern Amazonia: Observations and modelling results, *Theor. Appl. Climatol.*, *78*, 111–121.

Silva Dias, P. L., and J. Marengo (1999), Águas atmosféricas, in *Águas Doces do Brasil—Capital Ecológico Usos Multiplos, Exploração Racional e Conservacão da Cunha Rebouças*, edited by A. Rebouças, B. Braga Jr., and J. G. Tundizi, pp. 65–116, Inst. de Estud. Avançados da Univ. de São Paulo, São Paulo, Brazil.

Souza, E. P., N. O. Renno, and M. A. F. Silva Dias (2000), Convective circulations induced by surface heterogeneities, *J. Atmos. Sci.*, *57*, 2915–2922.

Strong, C., J. D. Fuentes, M. Garstang, and A. K. Betts (2005), Daytime cycle of low-level clouds and the tropical convective boundary layer in southwestern Amazonia, *J. Appl. Meteorol.*, *44*, 1607–1619.

Tokay, A., A. Kruger, W. F. Krajewski, P. A. Kucera, and A. J. P. Filho (2002), Measurements of drop size distribution in the

southwestern Amazon basin, *J. Geophys. Res.*, *107*(D20), 8052, doi:10.1029/2001JD000355.

Tompkins, A. M. (2001), Organization of tropical convection in low vertical wind shears: The role of cold pools, *J. Atmos. Sci.*, *58*, 1650–1672.

von Randow, C., et al. (2004), Comparative measurements and seasonal variations in energy and carbon exchange over forest and pasture in south west Amazonia, *Theor. Appl. Climatol.*, *78*, 5–26.

von Randow, C., B. Kruijt, A. A. M. Holtslag, and M. B. L. de Oliveira (2008), Exploring eddy-covariance and large-aperture scintillometer measurements in an Amazonian rain forest, *Agric. For. Meteorol.*, *148*, 680–690.

Williams, E., et al. (2002), Contrasting convective regimes over the Amazon: Implications for cloud electrification, *J. Geophys. Res.*, *107*(D20), 8082, doi:10.1029/2001JD000380.

Williams, E. R., S. G. Geotis, N. Renno, S. A. Rutledge, E. Rasmussen, and T. Rickenbach (1992), A radar and electrical study of tropical "hot towers," *J. Atmos. Sci.*, *49*, 1386–1395.

Wright, I. R., C. A. Nobre, J. Tomasella, H. R. da Rocha, J. M. Roberts, E. Vertamatti, A. Culf, R. C. S. Alvalá, M. G. Hodnett, and V. N. Ubarana (1996), Towards a GCM surface parameterization of Amazonia, in *Amazonian Deforestation and Climate*, edited by J. H. C. Gash et al., pp. 473–504, John Wiley, New York.

A. K. Betts, Atmospheric Research, 58 Hendee Lane, Pittsford, VT 05763, USA. (akbetts@aol.com)

J. C. P. Cohen, Departamento de Meteorologia, Universidade Federal do Pará, Belém, PA 66075-900, Brazil.

R. da Silva, UFPA-LBA Santarém, Rua Lauro Sodré, 1330, Alter do Chão, PA 68109-000, Brazil.

G. Fisch, Instituto de Aeronáutica e Espaço, São José dos Campos, SP 12228-904, Brazil.

D. R. Fitzjarrald, Atmospheric Sciences Research Center, University at Albany, State University of New York, Albany, NY 12203, USA.

M. A. F. Silva Dias, Department of Atmospheric Sciences, University of São Paulo, São Paulo, SP 05508-900, Brazil.

C. von Randow, Instituto Nacional de Pesquisas Espaciais, Sao Jose dos Campos, SP 12227-010, Brazil.